Origin of the Bright Photoluminescence of Thiolate-protected Gold Nanoclusters: Confined Structural Water Molecules as Real Emitters

Bo Peng, [1] Kun Zhang*[1,2,3]

[1] Shanghai Key Laboratory of Green Chemistry and Chemical Processes, College of Chemistry and Molecular Engineering, East China Normal University, Shanghai 200062, China;

[2] Laboratoire de chimie, Ecole Normale Supérieure de Lyon, Institut de Chimie de Lyon, Université de Lyon, 46 Allée d'italie, 69364 Lyon cedex 07, France;

[3] Shandong Provincial Key Laboratory of Chemical Energy Storage and Novel Cell Technology, School of Chemistry and Chemical Engineering, Liaocheng University, Liaocheng, 252059, Shandong, P. R. China.

* kzhang@chem.ecnu.edu.cn (K.Z.)

Abstract: The availability of a range of excited states has enriched zero-, one- and two-dimensional quantum nanomaterials with interesting luminescence properties, in particular for noble metal nanoclusters (NCs) as typical examples. But, the elucidation and origin of optoelectronic properties remains elusive. In this report, using widely used Au(I)-alkanethiolate complex (Au(I)-SRs, R = -$(CH_2)_{12}H$) with AIE characteristics as a model system, by judiciously manipulating the delicate surface ligand interactions at the nanoscale interface, together with a careful spectral investigations and an isotope diagnostic experiment of heavy water (D_2O), we evidenced that the structural water molecules (SWs) confined in the nanoscale interface or space are real emitter centers for photoluminescence (PL) of metal NCs and the aggregate of Au(I)-SRs complexes, instead of well-organized metal core dominated by quantum confinement mechanics. Interestingly, the aggregation of Au(I)-SRs generated dual fluorescence-phosphorescence emission and the photoluminescence intensity was independent on the degree of aggregation but showed strong dependency on the content and state of structural water molecules (SWs) confined in the aggregates. SWs are different from traditional hydrogen bonded water molecules, wherein, due to interfacial adsorption or spatial confinement, the p orbitals of two O atoms in SWs can form a weak electron interaction through spatial overlapping, which concomitantly constructs a group of interfacial states with π bond characteristics, consequently providing some alternative channels (or pathways) to the radiation and/or non-radiation relaxation of electrons. Our results provide completely new insights to understand the fascinating properties (including photoluminescence, catalysis and chirality, etc.) of other low-dimension quantum dots and even for aggregation-induced emission luminophores (AIEgens). This also answers the century old debate on whether and how water molecules emit bright color.

Introduction

Nano-materials, including metal nanoclusters (NCs)[1-5], carbon quantum dots[6, 7] and semiconductor quantum nanostructures[8], *etc.*, usually exhibited dramatically unique electronic and optical properties (such as molecule-like energy gaps[9-14], photoluminescence (PL)[1, 15-27], catalytic properties[28-36] and chirality[37-43], *etc.*) compared to that of bulky one.[44, 45] For instance, thiolate-protected gold NCs can achieve intense PL with quantum yield even up to 90%[46], which is much higher than that of bulk gold (10^{-10})[47]. The luminescent properties of thiolate-protected Au NCs was largely dictated by the composition of metal and ligand[48-50],

cluster size[48, 51], surface ligands architecture[52], cluster assembly structure[53], *etc*. Even though atomically precise Au NCs with molecule purity can be prepared and its structure was revealed at atomic resolution[54, 55], the elucidation on the origin of the optoelectronic properties of metal NCs is still diverse and even contradictory[56], and achieving a unified understanding of luminescent low-dimension quantum dots was far behind.

Non-luminescent chromophoric organics can achieve intense PL through aggregation, which was known as aggregate-induced emission (AIE).[57-59] The PL intensity of AIE luminophores (AIEgens) was dependent on the degree of aggregation, which intuitively attributed to the restraints on the intramolecular vibrations and rotations. Recently, this fascinating AIE effect was also observed in non-conjugated small organic molecules[60, 61] and metal-thiolate complex[52, 62-65]. We can conclude that both quantum size effect or AIE effect is not a personality for a certain type of materials or molecules but a common feature for luminescent materials, and metal-thiolate complexes bound on metallic core in good solvent or aggregated in the poor solvent can emit identical phosphorescence[52], which established a connection between quantum size effect and AIE effect. We would ask whether the common luminescent properties may not originated from the quantum dots or aggregates itself but a common species, such as ubiquitous water molecules suggested and investigated in our previous researches[66-71], adsorbed or confined in the nanoscale interface and/or space? Understanding the luminescent fundamentals of metal(I)-thiolate complexes with AIE characteristics can give better insight to both quantum size effect and AIE effect on luminescence for low-dimension quantum dots and AIEgens, respectively. Herein, a systematic and comprehensive investigation of luminescent Au(I)-alkanethiolate complexes with AIE characteristics were performed, the luminescent properties was susceptible to the ligand-metal ratio in the synthesis and external stimulus (pH, temperature, solvent and water molecules). The bright photoluminescence of ligand-protected gold nanoclusters or complexes was attributed to the behaviors of structural water molecules (SWs) confined in the nanoscale interface and/or space and its physical origin was discussed, which completely subverts the traditional cognitive and mechanic models for the understanding on the origin of PL of low-dimension quantum dot materials and AIEgens.

Results and discussion

Luminescent Au(I)-alkanethiolates (Au(I)-SRs, R = -$(CH_2)_{12}H$) oligomers can be facilely prepared by mixing ethanol solution of gold precursors ($HAuCl_4$) and thiol ligand (1-dodecanethiol, DT) at room temperature[72] (synthetic details in supporting information), as-obtained oligomers were labeled as Au(I)-SRs@xeqDT, in which x represented the added equivalents of DT (eq, equivalent to the moles of $HAuCl_4$). In a typical reduction reaction of $HAuCl_4$ by alkanethiol[73], as shown in the reaction 1, Au(III) was firstly reduced to Au(I) by two equivalents of alkanethiol and then as-formed Au(I) quickly bonded with another equivalent of alkanethiol to form Au(I)-SRs.

$$HAuCl_4 + 3\ RS\text{-}H \rightarrow 4\ HCl + Au^+\ SR^- + RS\text{-}SR \quad (1)$$

The stoichiometric reduction of $HAuCl_4$ and formation of Au(I)-SRs oligomers were confirmed by comparing the UV-vis absorption spectra of Au(I)-SRs@xeqDT stock solution. As shown in Figure 1a, with the increase of x from 0 to 3~4, the sharp absorption peak centered at 225 nm for $HAuCl_4$ was declined and companied with the generation and strengthening of one set of absorption peaks centered at 290 nm, 355 nm, and 400 nm (red stars*), implying the reduction of Au(III) and the formation of Au(I)-SRs oligomers. The assignment of these multiple absorption

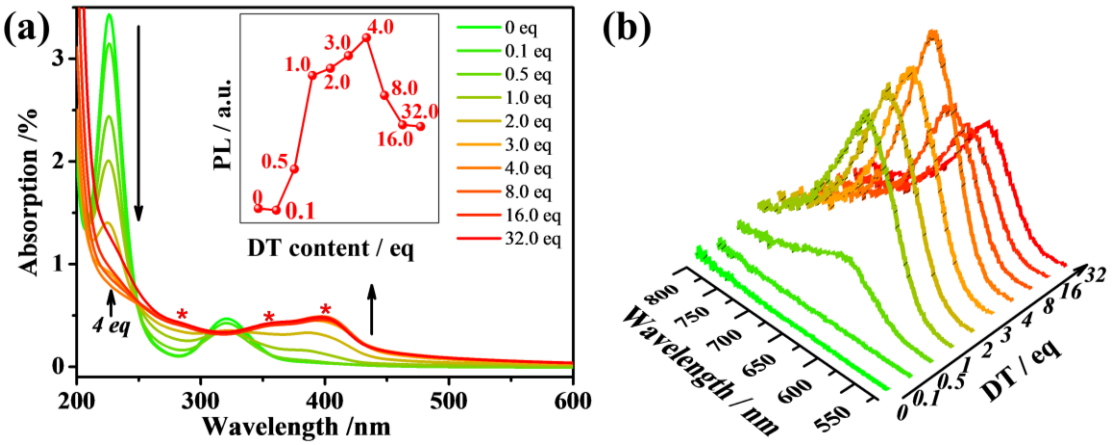

Figure 1. UV-vis absorption spectra (a) and photoluminescence spectra (b) of the mixture of $HAuCl_4$ and different equivalents of DT in the ethanol solution. Insert: relationship between PL intensity and DT content.

bands will be discussed later. No significant change in the absorption spectra was observed with an excessive addition of DT, only the absorption band centered at 230 nm, which featured for free DT molecules in ethanol solution (Figure S1), was intensified. Figure 1b shows the PL spectra of Au(I)-SRs@xeqDT oligomers solution, an emission band centered at 630 nm was generated upon addition of 0.5 eq DT, the PL intensity of Au(I)-SRs@xeqDT oligomers shows a volcano-type trend with the increase of added equivalents (x) of DT, when x was approached to the stoichiometric ration of reaction 1, the Au(I)-SRs@4eqDT showed strongest PL intensity, and a further increase in x resulted the decrease in PL intensity. As the Au(I)-SRs (R = $-(CH_2)_{12}H$) oligomers was either insoluble in the polar or non-polar solvents[72], the precipitated Au(I)-SRs oligomers can be regarded as an aggregate of Au(I)-SRs complexes and its PL followed the phenomena of AIE, this hypothesis will be verified in the following experiment results. Therefore, the further decrease in the PL intensity of Au(I)-SRs@xeqDT (x>4) could be attributed to the formation of shorter oligomers which was favored at high molar ratio of ligand to gold[74], as-formed shorter oligomers shows stronger affinity toward ethanol solvent and resulted comparative lower aggregated degree.

Intriguingly, the PL intensity of Au(I)@SRs oligomers showed a prominent pH-responsive effect, and this effect was different within these Au(I)-SRs@xeqDT oligomers. Three typical samples Au(I)-SRs@2eqDT, Au(I)-SRs@4eqDT and Au(I)-SRs@8eqDT, which represented as ligand-poor, ligand-moderate and ligand-rich oligomers solution, respectively, were selected to investigate the pH-dependent PL properties. Ten equal aliquots of Au(I)-SRs@xeqDT oligomers solution was prepared and added different equivalents (eq, equivalent to the moles of Au) of NaOH aqueous solution respectively (details in supporting information). According to the reaction 1, as-prepared stock solution was acidic due to the formation of four equivalents of HCl, the acidic stock solution gradually turned to basic with the dosing of NaOH and corresponding UV-vis absorption and PL spectra were recorded and shown in the Figure 2. The PL intensity of Au(I)-SRs@2eqDT increased with the increase of added equivalents of NaOH (Figure 2a and 2d insert), whereas, on the contrary, the red emission was gradually quenched for Au(I)-SRs@8eqDT when the solution turn to basic (Figure 2c and 2f insert). In the first case, the added amount of DT ligand (2 eq) was insufficient for the reduce of $HAuCl_4$ and the formation of Au(I)-SRs oligomers,

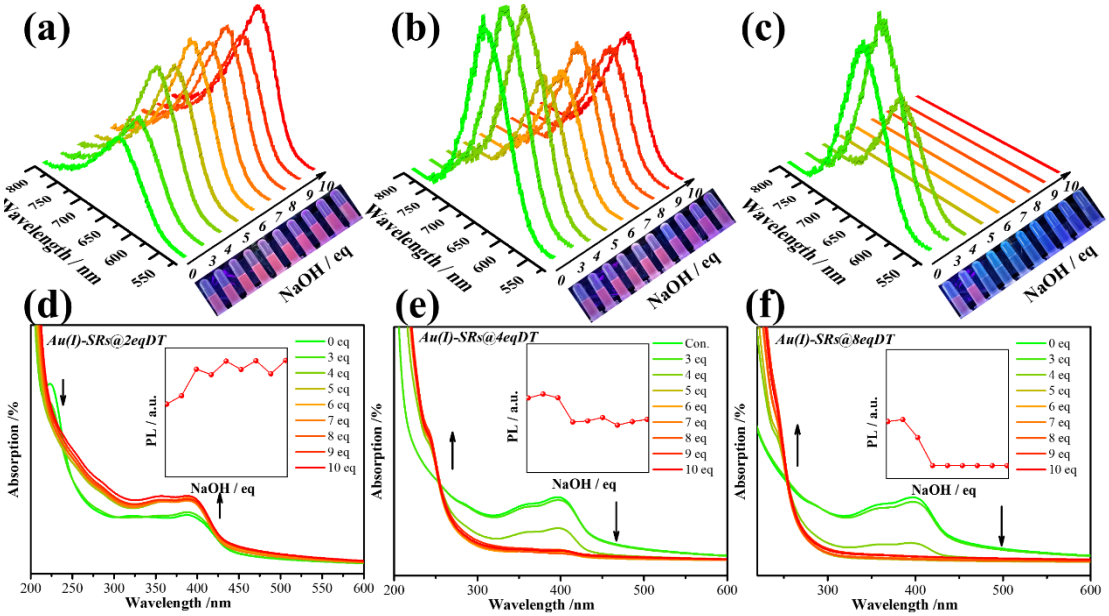

Figure 2. UV-vis absorption spectra (bottom plane) and photoluminescence spectra (top plane) of Au(I)-SRs@2eqDT (a,d), Au(I)-SRs@4eqDT (b, e) and Au(I)-SRs@8eqDT (c, f) with the dosing of different equivalents of NaOH. Insert: corresponding digital photographs under UV light (a, b and c) and relationship between PL intensity and added equivalents of NaOH (b, e and f).

implied by the obvious absorption peaks at 225 nm for $HAuCl_4$ in the absorption spectrum (Figure 2d, downward arrow). Therefore free $HAuCl_4$ precursors could be reduced to metallic Au(0) with the introducing of NaOH, consistent with the decline of the 225 nm absorption peaks after dosing NaOH and the observations of TEM (Figure S2). As-formed Au(0) core stapled Au(I)-SRs complexes on the surface and resulted the strengthen of PL intensity as well as the absorption band at 250~400 nm (Figure 2d, upward arrow). In the latter case, $HAuCl_4$ precursors were completely reduced and transformed to the Au(I)-SRs by DT as suggested in Figure 1a, under alkaline solution, the absorption bands at 250~400 nm featured for Au(I)-SRs oligomers was disappeared (Figure 2f, downward arrow) and the absorption peak at ~230 nm featured for free DT molecules was intensify (Figure 2f, upward arrow), which suggested that the OH^- in the solution could replace partial DT ligand and coordinate with Au(I),which resulted the dissociation of Au(I)-SRs oligomers. The dissolve of concentrated Au(I)-SRs oligomers precipitate in alkaline solution can be directly observed in digital photographs (Figure S3). Therefore, the partial decrease in PL intensity observed for Au(I)-SRs@4eqDT was synergistic effect of the formation of metallic Au NCs and the dissociation of Au(I)-SRs oligomers (Figure 2b and 2e). To verify this hypothesis, Au(I) in the Au(I)-SRs@8eqDT oligomers were partially reduced into metallic Au(0) through heat treatment, which was confirmed by the observations of TEM (Figure S4). The PL intensity largely increased with the increase of temperature during the synthesis (Figure S5), which was similar to that of Au(I)-SRs@2eqDT oligomers solution with the dosing of NaOH, and the PL intensity of as-obtained Au NCs solution synthesized at elevated temperature such as 80 ℃ was only partial decreased after dosing NaOH, which was similar to that of Au(I)-SRs@4eqDT oligomers solution after dosing NaOH. Therefore it can be concluded that the luminescent properties of Au(I)-SRs@xeqDT oligomers was the consequence of the aggregation of Au(I)-SRs complexes, showing an AIE effect, and metallic core can be regarded as an aggregation trigger

that stapled Au(I)-SRs together. In most of case, the pH-dependent luminescent properties of Au NCs with AIE characteristics was typically attributed to the pH-dependent charge state or solvophilicity of protective ligand[75, 76]. Herein, the pH-dependent luminescent properties of Au(I)-SRs was more likely ascribed to the pH-dependent structural variation of Au(I)-SRs due to the binding interaction between Au(I) and OH^-.

Controllable re-aggregation of soluble Au(I)-SRs complexes in the ethanol solution was achieved using a solvent-induced aggregation method triggered by addition of water as a poor solvent, and the effect of added equivalents of NaOH on AIE was investigated. To get a better well-resolved absorption and PL spectra of aggregates solution, the Au(I)-SRs@8eqDT stock solution was concentrated ten times compared to that in Figure 2c and 2f, after adding different equivalents of NaOH, the obtained solution was labeled as Au(I)-SRs@yeqNaOH, in which y represented the added equivalents of NaOH. Each of Au(I)-SRs@yeqNaOH (y=4, 8, 16 and 32) solutions and Au(I)-SRs@8eqDT oligomers solution as reference was divided into ten equal aliquots and diluted 10 times by adding mixed solvents with different volume fraction of R_w (R_w=Vol_{water}/$Vol_{water+ethanol}$) respectively (details in supporting information), and corresponding UV-vis absorption and emission spectra were recorded and shown in the Figure 3 and Figure S6. In the case of Au(I)-SRs oligomers solution (Figure S6), the aggregates of Au(I)-SRs oligomers only showed a parent red emission at 630 nm and no other emission color was observed with the

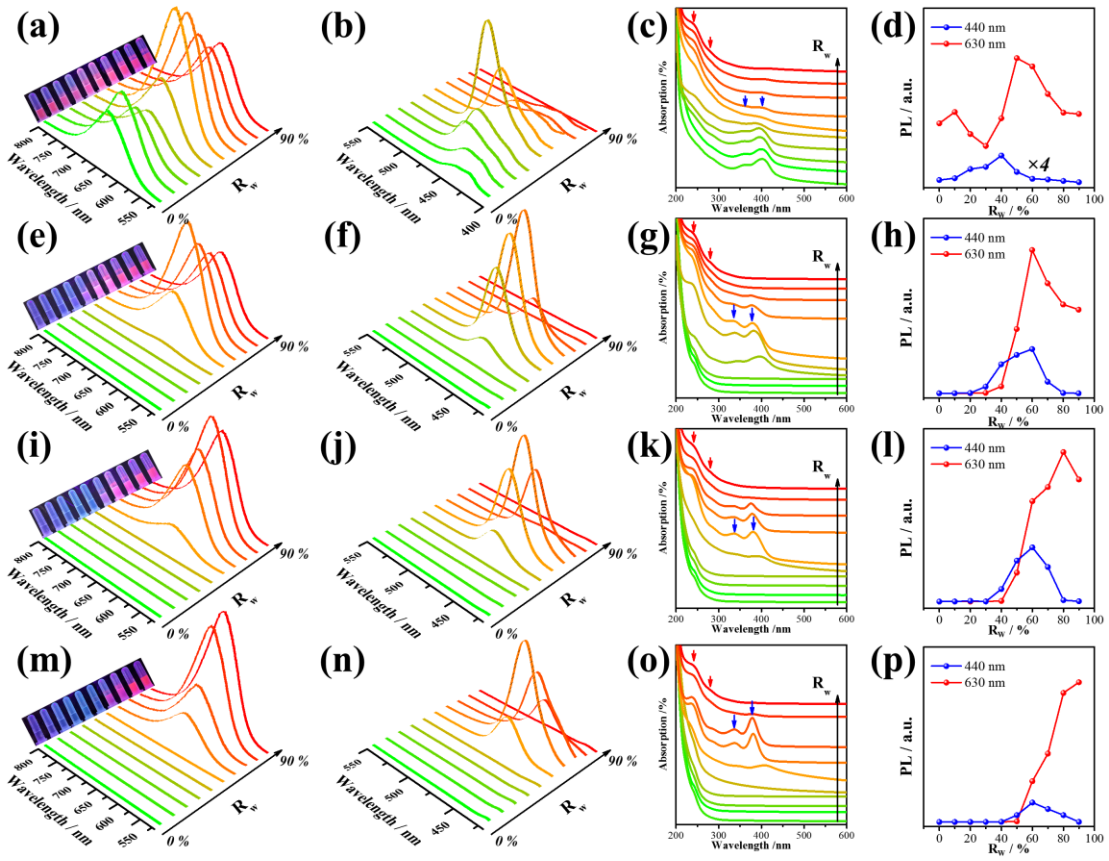

Figure 3. Photoluminescence (630 nm and 460 nm) spectra, UV-vis absorption spectra and the relationship between PL (630 nm and 460 nm) intensity and R_w of Au(I)-SRs@4eqNaOH (a-d), Au(I)-SRs@8eqNaOH (e-h), Au(I)-SRs@16eqNaOH (i-l) and Au(I)-SRs@32eqNaOH (m-p) in mixed solvent with different R_w. Insert: corresponding digital photographs under UV light (a, e, i and m).

increase of R_w. As Au(I)-SRs oligomers cannot be well dispersed in the aqueous solution and easily stuck to the vessel (Figure S6c), corresponding absorption and PL intensity was inaccurate but showed an overall trend that firstly increased and then decreased with the increase of R_w (Figure S6a and b). For the soluble Au(I)-SRs complexes, interestingly, dual fluorescence-phosphorescence emission bands centered at 460 nm and 630 nm were generated through the solvent-induced aggregation, in which red emission at 630 nm exhibited a large stokes shift (λ_{ex}=290 nm, Figure S7a) and long lifetime (~5.5 us, Figure S8a) as a characteristic for phosphorescence, and blue emission at 460 nm exhibited a small stokes shift (λ_{ex}=390 nm, Figure S7b) and short lifetime (~2.9 ns, Figure S8b) as a characteristic for florescence. Besides, the PL intensity shows a volcano-like trend with the increase of R_w or degree of aggregation: at a critical volume fraction of water (R_w*), the aggregates of Au(I)-SRs complexes achieved strongest PL intensity and R_w* was changeful and highly related to the added equivalents of NaOH in the solution. In the case of Au(I)-SRs@4eqNaOH, the solution was a mixture of Au(I)-SRs oligomers and soluble complexes, therefore, weak red emission was observed in the ethanol solution and the evolution of the absorption and PL intensity with the increase of R_w was similar to that of Au(I)-SRs oligomers (Figure S6) when R_w was lower than 30%. When R_w surpassed 30%, the red emission centered at 630 nm was gradually intensified and reached a maximum at R_w^* 50%, a further increase in R_w resulted a decrease in the PL intensity of red emission (Figure 3a and 3d). Besides, a new emission band centered at 460 nm was generated when R_w is higher than 10% and reached a maximum at R_w^* 40%, a further increase in R_w resulted a decrease and quenching in PL intensity of blue emission (Figure 3b and 3d). With respect to Au(I)-SRs@8eqNaOH, Au(I)-SRs@16eqNaOH and Au(I)-SRs@32eqNaOH, the lowest R_w for the generation of red emission was increased from 30%, 40% to 50% and R_w^* for red emission was estimated as 60%, 80% and 90%, respectively, showing a positive correlation to the equivalents of NaOH. Similarly, the lowest R_w for the generation of blue emission was increased from 30%, 40% to 50%, respectively, but R_w* for the blue emission was all the same (60%), and notably, all the blue emission was quenched at high R_w.

The evolution of the absorption signals (Figure 3g, 3k and 3o) can be well correlate to that of PL intensity of two emission bands, the generation, strengthening and decline of two sets of absorption peaks centered at *ca.* 260 nm and 290 nm (red arrow), and *ca.* 350 nm and 390 nm (blue arrow) followed the similar trend to the evolution of the red and blue emission band, respectively. Besides, it was worthwhile noting that a broad absorption band centered at 400 nm, which was similar to that of as-formed Au(I)-SRs oligomers (Figure 1a), was firstly generated and suffered blue-shift, intensify and disappearance with the increasing of R_w. Therefore, these variable absorption peaks cannot directly assigned to the electronic structure of Au(I)-SRs oligomers or the aggregates of Au(I)-SRs complexes since the interactions of Au(I)-S bonding in both complex and oligomer are always there.[11, 63] Not only the amount of NaOH, but also the concentration of precursors solution (Figure S9) and the amount of DT (Figure S10) in the synthesis of Au(I)-SRs oligomers significantly affect the dynamic evolution of these interesting absorption bands and PL intensity, which is against the fundamental principle of AIE mechanism with a model of the limitation of molecule mobility, and also which cannot be answered by the conventional metal quantum confinement effect and ligand-to-metal charge transfer (LMCT) or ligand-to-metal-metal charge transfer (LMMCT) emphasized the metallophilic interactions.[63]

Without organic templates, silver NCs confined in the rigid micropores of zeolites exhibited

similar dual fluorescence-phosphorescence emission, in which higher energy emission band possessed a short lifetime (ns scale) and lower one possessed a long lifetime (μs scale). The emission properties can be tuned by the solvent[68], thermal annealing treatment[77] and cations[19, 78, 79], *etc*. which was highly related to the hydration state of silver NCs[20, 80], and the emission was unambiguously attributed to the behavior of structural water molecules (SWs) confined in nanoscale interface and/or space [67-71]. Based on the fundamentals of SWs, these elusive results as above discussed can be well understood. As illustrated in the Figure 4a, firstly, free OH^- in the solution was bonded with Au(I) and resulted the dissociation of Au(I)-SRs oligomers as well as SWs (Figure 4a, stage I and II). The soluble hydrophobic Au(I)-SRs complexes began to aggregation with the introducing of poor solvent (water), the structural evolution of Au(I)-SRs aggregates was imaged by the TEM observation (Figure S11) in which the structure of Au(I)-SRs transformed from highly dispersed Au(I)-SRs complexes to loose and larger aggregates and then to small and dense aggregates with the increasing of R_w. At low R_w, loose and large aggregates was formed and recreated a soft nanoscale interface benefited for the formation of two types of SWs through space interaction[67-69, 81] (Figure 4a, stage III). Type I SWs are the water molecules bonded with the Au(I) through strong coordination interaction and type II SWs are the water molecules bonded with adsorbed H_2O or OH^- through weak hydrogen-bonding interaction, which resulted the red and blue emission respectively. Small and dense aggregates, in which the hydrophobic carbon chain was entangled together, was formed at high R_w and resulted the complete remove of the type II SWs and partially maintained the type I SWs on the rigid interface through hydrophobic interaction (Figure 4a, stage IV), which is corresponding to the quenching of blue emission and the decline of red emission at high R_w. When the dosed equivalents (Figure 3) or concentration (concomitantly changed with the concentration of precursors solution, Figure S9) of NaOH was increased, more OH^- could bonded with Au(I)-SRs and endowed the complex with larger negative charge density, the electrostatic repulsion between Au(I)-SRs complexes resisted the aggregation and thus high R_w was needed for

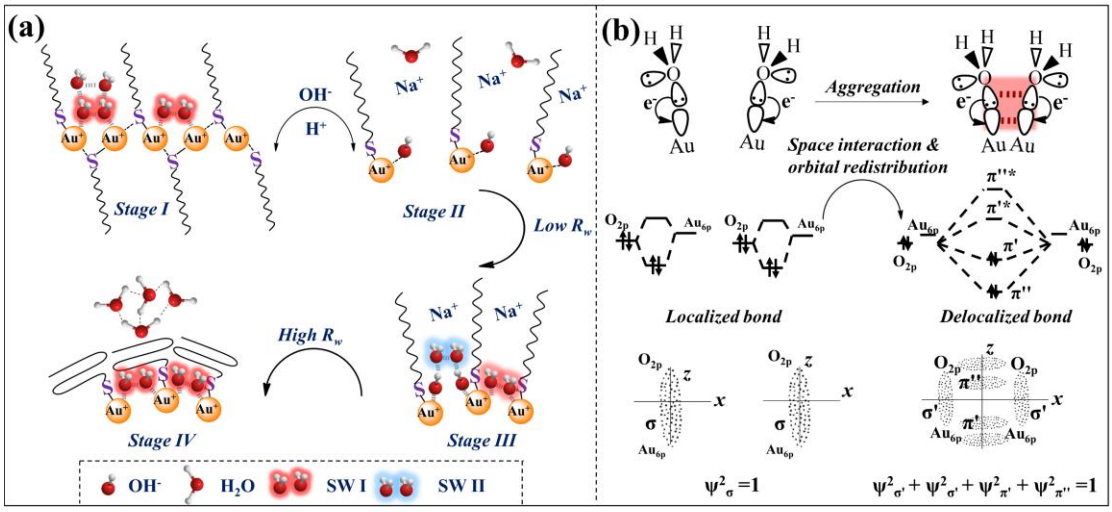

Figure 4. (a) Schematic illustration of the evolution of luminescent Au(I)-SRs oligomer (stage I: the formation of Au(I)-SRs oligomers; stage II: the dissociation of Au(I)-SRs oligomers after dosing NaOH; stage III: the loose aggregates of Au(I)-SRs complexes in the mixed solvent with low R_w; stage III: the dense aggregates of Au(I)-SRs complexes in the mixed solvent with low R_w); (b) Schematic illustration of the formation mechanism of luminescent SWs.

the formation of stable SWs with bright PL. When hydrophobic DT ligand was increased in the synthesis (Figure S10), the removal of weak bonded water molecules was advanced due to the co-aggregation of Au(I)-SRs complexes and substantial hydrophobic DT molecules before the formation of stable SWs, which resulted the weak blue emission and successive increase of red emission intensity with the increase of R_w.

So if confined SWs were the true emitters, what is the physical origin of the new electronic structure of that and how to tailor the color of emission? The distance and stability of water molecules in the bulk solution is determined by the hydrogen bonding interaction and the rate of proton shuttling in the H-bond networks [82]. A further approaching of adjacent water molecules could lead to the increase of potential energy due to the electrons repulsion, which was not stable and cannot spontaneously proceed. While, the SWs confined at the nanoscale interface and/or space shows more peculiar physic-chemical properties due to the specific distance and spatial orientation between paired SWs, wherein the potential energy is increased compared to that of water molecules in the bulk solution but can be compensated by the adsorption energy (such as the coordination and hydrogen bonding interaction between water molecules and adsorption sites) and interface energy (such as the hydrophilic-hydrophobic interaction between water molecules and ligands). In addition, such an intimate contact and matched spatial orientation between paired water molecules would induce the re-combinations of the localized chemical bonds through space interaction on the molecule level [81], yielding a new set of surface states by the delocalization of valence electron of O-H and/or O-M localized chemical bonds (O atoms from interfacial adsorbed SWs and M denotes the metals). This weak interaction is analogous to that of intra-molecular electron interaction (such as π/π conjugation effect, p/π conjugation effect and σ/π conjugation effect, *etc.*), and the electronic structure of interacted chemical bonds can be also approximately derived from the molecular orbital theory.

Taking type I SWs for an example (Figure 4a), the 2p orbital with paired electrons of O atoms in water firstly formed an localized coordination bonds with the empty 6p orbital of Au(I), with the approaching of the adjacent Au(I)-H_2O species through solvent-triggered aggregation, two type of electrons interaction between adjacent O_{2p} orbitals and adjacent Au_{6p} orbitals can be derived through the orbital liner combination, which possess similar properties of π bond with the 'side by side' interaction pattern (Figure 4b, in the bottom). These interfacial states are similar to the transition states for chemical reaction with dynamic and interfacial delocalized features which was denoted as σ' bond for O_{2p}-Au_{6s}, π' bond for Au_{6p}-Au_{6p} and π'' bond for O_{2p}-O_{2p} to distinguish the localized chemical bond, respectively. In other words, the coordination bonds between O_{2p} and Au_{6s} was not completely broken and the O_{2p}-O_{2p} and Au_{6p}-Au_{6p} chemical bonds was not completely formed. Obviously, the bonding strength of σ' bonds perpendicular to the interface determines the energy and profile of π' and π'' bonds parallel to the interface direction, which regulates the spectral characteristics of steady-state absorption and emission spectra of Au NCs or aggregates (Figure 3). Differing from the *d*-band center theory for transition metals, a simple physical faramework named as the "p band intermidate states (PBIS)" model is proposed to illuminate the principles for modulating the PL properties of low-dimensional quantum nanodots, we also called it *p*-band model for simplicity[66, 69]. Owing to the transient occupancy of p orbitals, the bonding electrons was delocalized at four region of electron interaction (two σ' bond, one π' bond and one π'' bond) as shown in the schematic electron cloud diagram (Figure 4b, bottom), imaging the electron pool at the nanosale interface. Importantly note that, the sum of the

probability density (ψ^2) of electron appearance at four interfacial bonding region is equal to 1 ($\psi^2_{\sigma'} + \psi^2_{\sigma'} + \psi^2_{\pi'} + \psi^2_{\pi''} = 1$) according to quantum mechanics, and the ψ^2 of each part can be tuned by the distance, symmetry or space orientation and the energy structure of ligand and metal according to bonding principle of molecular orbital theory. Recently, we demonstrated that, the formed transient states by *p*-band model could acts as alternative channels for surface electron and proton transfer in the reduction and oxidation reactions[83-85], which could answer the nature of surface states and/or surface bonds at heterogeneous catalysis interface[86].

Now we can give a unified interpret for the luminescent properties in the community of ligand protected metal NCs. We deduced that the electronic interaction with the properties of π bonding between adjacent O_{2p} orbitals of water (π'' bond) is the origin of the emission of Au(I)-SRs. For this regard, the type I SWs showed a strong interaction between O_{2p} and Au_{6p} (σ' bond) and more rigid spatial orientation, which resulted small overlapping of O_{2p}-O_{2p} orbitals (π'' bond) and showed a lower energy emission band at 630 nm. Following the same working principle, large overlapping of O_{2p}-O_{2p} orbitals in more mobile type II SWs occurred due to the dense packing of hydrophobic ligand, resulting in the higher energy emission with a short wavelength of *ca.* 460 nm. This also answered that, the overlapping degree of O_{2p}-O_{2p} p orbitals was highly dependent on the aggregated degree, determining the generation, blue-shift and intensity of the absorption bands centered at 300-400 nm in Figure 3k and 3o. It is importantly noted that, even though the multiple type II SWs could be formed on the nanoscale interface, only stable one can emit intense fluorescence, that is why Au(I)-SRs oligomers exhibited a board absorption at 300-400 nm but no blue emission. The concept of SWs as an emitter center not only provides new insights to understand the fascinating properties (including luminescence, catalysis and chirality, *etc.*) of low-dimension quantum dots and molecular aggregates,[83-85] but also give a new fundamental understanding on the origin of metallophilic interactions between the closed-shell metal centers.[87, 88]

More direct experimental evidence on the SWs as an emitter center is coming from the diagnostic experiment that the luminescent properties of Au(I)-SRs complexes solution are determined by the presence of water molecules. Au(I)-SRs complexes were synthesized using a modified Brust-Schiffrin phase-transfer method[89] (Figure 5a). Firstly, tetra-n-octylammonium bromide (TOAB) was used as phase transfer catalysts to transfer the $AuCl_4^-$ from aqueous phase to toluene phase, the yellow $HAuCl_4$ aqueous solution turn to colorless and the colorless toluene phase turn to deep red due to the dissolve of $AuCl^-TOA^+$. The water phase was discarded and a certain amount of dried 4A zeolite was added into the toluene phase to completely remove residue water. Excessive DT molecules was then added to reduce $HAuCl_4$ and form Au(I)-SRs complexes, the red toluene phase was turn to colorless, suggesting the complete reduction of $AuCl_4^-$ by DT (synthetic details in supporting information). Intriguingly, the Au(I)-SRs complexes was non-luminescent but once trace amount of water was added, the red emission centered at 630 nm (Figure 5c) as well as the absorption bands (Figure 5b) centered at 300-400 nm was generated and intensified with the increasing of water volume. Also, it can be observed that the toluene phase turn to cloudy after the introducing of water (Figure 5b, insert), implying the formation of Au(I)-SRs aggregates, the aggregates provide a confined interface, which are beneficial for the formation of SWs as above discussed (Figure 4b, top). Very interestingly, when replacing thewater (H_2O) by heavy water (D_2O) in the toluene phase, the PL intensity was further intensified, but without any peak shifts (Figure 5d), which was probably attributed to the limited intra- and inter-

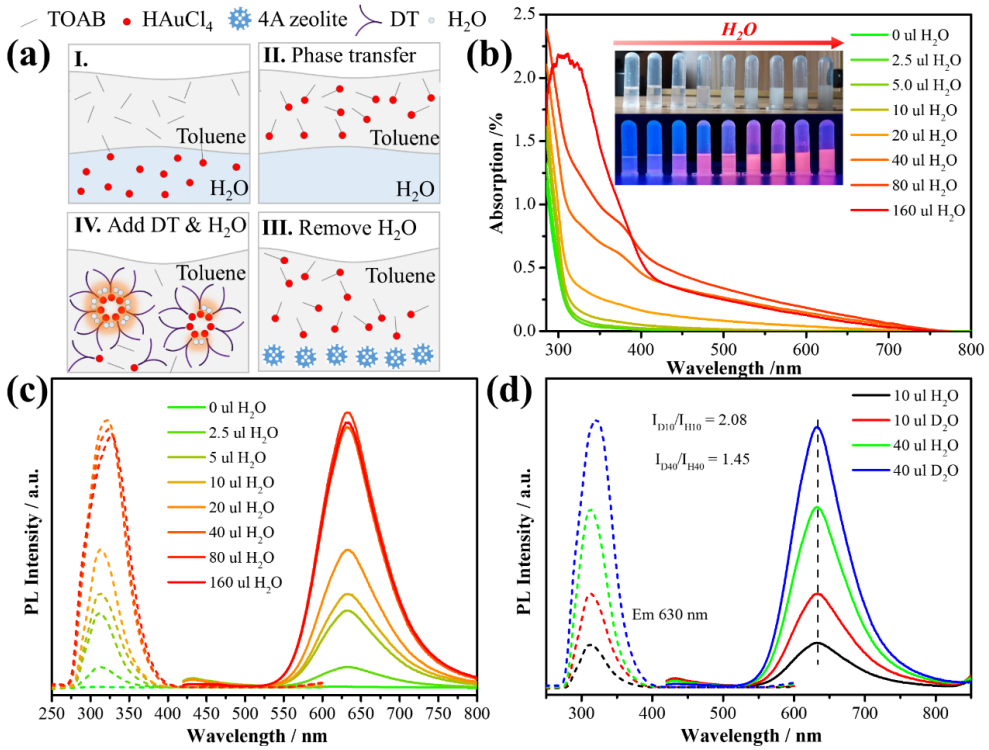

Figure 5. (a) Schematic illustration of the formation of luminescent Au(I)-SRs through modified Brust-Schiffrin method; UV-vis absorption spectra (b) and photoluminescence spectra (c) of dosing different volume of water in the Au(I)-SRs toluene solution; (d) comparison the emission properties of Au(I)-SRs in the toluene solution with the dosing of H_2O and D_2O. Insert (b): Digital photographs of Au(I)-SRs toluene solution with the dosing of different volume of water under visible (top row) and UV (bottom row) light.

molecular rotation and vibration of heavy water molecule and slowed proton transfer rate between two paired O atoms in SWs, compared to that of water molecules since the non-radiative decay channels are blocked [68, 69]. These observations further confirmed that SWs was the true emitters for luminescent Au(I)-SRs.

Conclusion

In summary, we thoroughly studied the electronic and optical properties of Au(I)-SRs oligomers through tuning the ligand-metal ratio in the synthesis and imposing external stimulus (pH, temperature, solvent and water molecules). The bright photoluminescence of ligand-protected gold nanoclusters or complexes was attributed to the behaviors of structural water molecules (SWs) confined in the nanoscale interface and/or space. Solid experimental evidence shows that: (i) Au(I)-SRs bound on metallic Au(0) core in good solvent (ethanol) or aggregated in poor solvent (water) can emit identical PL; (ii) the aggregation of Au(I)-SRs generated tunable dual fluorescence-phosphorescence emission and their PL intensity was independent on the agree of aggregation; (iii) water molecules showed an on/off and prominent isotope effect on the PL intensity of luminescent Au(I)-SRs oligomers. We suggested that SWs confined in the nanoscale interface and/or space could generate new delocalized electronic interaction between adjacent water molecule through space interaction which regulated the tunable electronic structure and emission color. The fundamentals of SWs mechanism can give a unified understanding of quantum size effect and AIE effect on luminescent properties. And we believed that the concept of SWs, a strong electronic interaction at interface, is a common features for molecules confined in

the nanoscale interface and/or space can provide new insight to understand and rationally regulate the fascination properties (such as luminescence, catalysis and chirality, *etc.*) of low-dimension quantum dots and molecular aggregates[90, 91].

Author Contributions

KZ conceived and directed the project. BP performed the main experiment. KZ and BP proposed the structural water molecules (SWs) as real emitters for the elucidation of origin of PL emission of metal NCs, and co-designed the figures and wrote the manuscript. All authors have read and agreed to the published version of the manuscript.

Acknowledgments

This research was funded by the NSFC (22172051, 21872053, and 21573074), the Science and Technology Commission of Shanghai Municipality (19520711400), the Open Project Program of Academician and Expert Workstation, Shanghai Curui Low-Carbon Energy Technology Co., Ltd., and the JORISS program. K.Z. thanks ENS de Lyon for a temporary position as an invited professor in France.

Reference

1. Zheng, J., P.R. Nicovich, and R.M. Dickson, *Highly fluorescent noble-metal quantum dots.* Annu. Rev. Phys. Chem., 2007. **58**: p. 409-31.
2. Yau, S.H., O. Varnavski, and T.G. III, *An Ultrafast Look at Au Nanoclusters.* Acc. Chem. Res., 2013. **46**: p. 1506–1516.
3. Chakraborty, I. and T. Pradeep, *Atomically Precise Clusters of Noble Metals: Emerging Link between Atoms and Nanoparticles.* Chem. Rev., 2017. **117**(12): p. 8208-8271.
4. Jin, R., et al., *Atomically Precise Colloidal Metal Nanoclusters and Nanoparticles: Fundamentals and Opportunities.* Chem. Rev., 2016. **116**(18): p. 10346-413.
5. Jin, R., *Quantum sized, thiolate-protected gold nanoclusters.* Nanoscale, 2010. **2**(3): p. 343-62.
6. Baker, S.N. and G.A. Baker, *Luminescent carbon nanodots: emergent nanolights.* Angew. Chem., Int. Ed., 2010. **49**(38): p. 6726-44.
7. Jiang, K., et al., *Red, green, and blue luminescence by carbon dots: full-color emission tuning and multicolor cellular imaging.* Angew. Chem. Int. Ed. Engl., 2015. **54**(18): p. 5360-3.
8. Alivisatos, A., *Semiconductor clusters, nanocrystals, and quantum dots.* Science, 1996. **271**: p. 933-937.
9. Schaaff, T.G., et al., *Isolation of Smaller Nanocrystal Au Molecules: Robust Quantum Effects in Optical Spectra.* J. Phys. Chem. B, 1997. **101**: p. 7885-7891.
10. Lee, D., et al., *Electrochemistry and Optical Absorbance and Luminescence of Molecule-like Au38 Nanoparticles.* J. Am. Chem. Soc., 2004. **126**: p. 6193-6199.
11. Negishi, Y., K. Nobusada, and T. Tsukuda, *Glutathione-Protected Gold Clusters Revisited: Bridging the Gap between Gold(I)-Thiolate Complexes and Thiolate-Protected Gold Nanocrystals.* J. Am. Chem. Soc., 2005. **127**: p. 5261-5270.
12. Walter, M., et al., *A unified view of ligand-protected gold clusters as superatom complexes.* Proc. Natl. Acad. Sci. USA, 2008. **105**(27): p. 9157-62.
13. Zhu, M., et al., *Correlating the Crystal Structure of A Thiol-Protected Au25 Cluster and Optical Properties.* J. Am. Chem. Soc., 2008. **130**: p. 5883-5885.
14. Bellina, B., et al., *Structural and Optical Properties of Isolated Noble Metal–Glutathione Complexes: Insight into the Chemistry of Liganded Nanoclusters.* J. Phys. Chem. C, 2011.

115(50): p. 24549-24554.
15. Zheng, J., C. Zhang, and R.M. Dickson, *Highly fluorescent, water-soluble, size-tunable gold quantum dots.* Phys. Rev. Lett., 2004. **93**(7): p. 077402.
16. Zheng, J., et al., *Different sized luminescent gold nanoparticles.* Nanoscale, 2012. **4**(14): p. 4073-83.
17. Yu, Y., et al., *Identification of a highly luminescent Au22(SG)18 nanocluster.* J. Am. Chem. Soc., 2014. **136**(4): p. 1246-9.
18. Peyser, L.A., et al., *Photoactivated Fluorescence from Individual Silver Nanoclusters.* Science, 2001. **291**: p. 103-106.
19. Cremer, G.D., et al., *Characterization of Fluorescence in Heat-Treated Silver-Exchanged Zeolites.* J. Am. Chem. Soc., 2009. **131**: p. 3049-3056.
20. Grandjean, D., et al., *Origin of the bright photoluminescence of few-atom silver clusters confined in LTA zeolites.* Science, 2018.
21. Fenwick, O., et al., *Tuning the energetics and tailoring the optical properties of silver clusters confined in zeolites.* Nat. Mater., 2016. **15**(9): p. 1017-22.
22. Kang, X. and M. Zhu, *Tailoring the photoluminescence of atomically precise nanoclusters.* Chem. Soc. Rev., 2019. **48**(8): p. 2422-2457.
23. Chen, Y., et al., *Photoemission Mechanism of Water-Soluble Silver Nanoclusters: Ligand-to-Metal–Metal Charge Transfer vs Strong Coupling between Surface Plasmon and Emitters.* J. Am. Chem. Soc., 2014. **136**(5): p. 1686-1689.
24. Ziefuss, A.R., et al., *Photoluminescence of Fully Inorganic Colloidal Gold Nanocluster and Their Manipulation Using Surface Charge Effects.* Adv. Mater., 2021. **33**(31): p. 2101549.
25. Wilcoxon, J.P. and J.E. Martin, *Photoluminescence from nanosize gold clusters.* J. Chem. Phys., 1998. **108**: p. 9137-9143.
26. Bigioni, T.P. and R.L. Whetten, *Near-Infrared Luminescence from Small Gold Nanocrystals.* J. Phys. Chem. B, 2000. **104**: p. 6983-6986.
27. Huang, T. and R.W. Murray, *Visible Luminescence of Water-Soluble Monolayer-Protected Gold Clusters.* J. Phys. Chem. B, 2001. **105**: p. 12498-12502.
28. Yan, J., B.K. Teo, and N. Zheng, *Surface Chemistry of Atomically Precise Coinage-Metal Nanoclusters: From Structural Control to Surface Reactivity and Catalysis.* Acc. Chem. Res., 2018. **51**(12): p. 3084-3093.
29. Fang, J., et al., *Recent advances in the synthesis and catalytic applications of ligand-protected, atomically precise metal nanoclusters.* Coord. Chem. Rev., 2016. **322**: p. 1-29.
30. Luo, Z., A.W. Castleman, and S.N. Khanna, *Reactivity of Metal Clusters.* Chem. Rev., 2016. **116**(23): p. 14456-14492.
31. Wang, Y., et al., *Atomically Precise Alkynyl-Protected Metal Nanoclusters as a Model Catalyst: Observation of Promoting Effect of Surface Ligands on Catalysis by Metal Nanoparticles.* J. Am. Chem. Soc., 2016. **138**(10): p. 3278-3281.
32. Tsunoyama, H., et al., *Effect of Electronic Structures of Au Clusters Stabilized by Poly(N-vinyl-2-pyrrolidone) on Aerobic Oxidation Catalysis.* J. Am. Chem. Soc., 2009. **131**: p. 7086-7093.
33. Wan, X.-K., et al., *Ligand effects in catalysis by atomically precise gold nanoclusters.* Sci. Adv., 2017. **3**: p. e1701823.
34. Zhang, Q.-F., X. Chen, and L.-S. Wang, *Toward Solution Syntheses of the Tetrahedral Au20*

Pyramid and Atomically Precise Gold Nanoclusters with Uncoordinated Sites. Acc. Chem. Res., 2018. **51**(9): p. 2159-2168.

35. Zhu, Y., et al., *Atomically precise Au25(SR)18 nanoparticles as catalysts for the selective hydrogenation of alpha,beta-unsaturated ketones and aldehydes.* Angew. Chem. Int. Ed. Engl., 2010. **49**(7): p. 1295-8.
36. Cai, X., et al., *Structural Relaxation Enabled by Internal Vacancy Available in a 24-Atom Gold Cluster Reinforces Catalytic Reactivity.* J. Am. Chem. Soc., 2020. **142**(9): p. 4141-4153.
37. Knoppe, S. and T. Bürgi, *Chirality in Thiolate-Protected Gold Clusters.* Acc. Chem. Res., 2014. **47**(4): p. 1318-1326.
38. Xia, Y., Y. Zhou, and Z. Tang, *Chiral inorganic nanoparticles: origin, optical properties and bioapplications.* Nanoscale, 2011. **3**(4): p. 1374.
39. Moshe, A.B., D. Szwarcman, and G. Markovich, *Size Dependence of Chiroptical Activity in Colloidal Quantum Dots.* ACS Nano, 2011. **5**: p. 9034-9043.
40. Li, Y., et al., *Chirality and Surface Bonding Correlation in Atomically Precise Metal Nanoclusters.* Adv. Mater., 2020. **32**(41): p. 1905488.
41. Xiao, L., et al., *Novel properties and applications of chiral inorganic nanostructures.* Nano Today, 2020. **30**: p. 100824.
42. Shen, J.-S., et al., *Metal–Metal-Interaction-Facilitated Coordination Polymer as a Sensing Ensemble: A Case Study for Cysteine Sensing.* Langmuir, 2010. **27**(1): p. 481-486.
43. Russier-Antoine, I., et al., *Chiral supramolecular gold-cysteine nanoparticles: Chiroptical and nonlinear optical properties.* Prog. Nat. Sci. Mater. Int., 2016. **26**(5): p. 455-460.
44. Roduner, E., *Size matters: why nanomaterials are different.* Chem. Soc. Rev., 2006. **35**(7): p. 583-592.
45. Daniel, M.-C. and D. Astruc, *Gold Nanoparticles: Assembly, Supramolecular Chemistry, Quantum-Size-Related Properties, and Applications toward Biology, Catalysis, and Nanotechnology.* Chem. Rev., 2004. **104**: p. 293-346.
46. Chang, H., et al., *Highly Fluorescent Gold Cluster Assembly.* J. Am. Chem. Soc., 2021. **143**(1): p. 326-334.
47. Mooradian, A., *Photoluminescence of Metals.* Phys. Rev. Lett., 1969. **22**(5): p. 185-187.
48. Zheng, J. and R.M. Dickson, *Individual Water-Soluble Dendrimer-Encapsulated Silver Nanodot Fluorescence.* J. Am. Chem. Soc., 2002.
49. Wu, Z. and R. Jin, *On the ligand's role in the fluorescence of gold nanoclusters.* Nano Lett., 2010. **10**(7): p. 2568-73.
50. Zhou, C., et al., *Luminescent Gold Nanoparticles with Mixed Valence States Generated from Dissociation of Polymeric Au(I) Thiolates.* J. Phys. Chem. C, 2010. **114**: p. 7727–7732.
51. Liu, J., et al., *Luminescent Gold Nanoparticles with Size-Independent Emission.* Angew. Chem. Int. Ed., 2016. **55**(31): p. 8894-8.
52. Luo, Z., et al., *From aggregation-induced emission of Au(I)-thiolate complexes to ultrabright Au(0)@Au(I)-thiolate core-shell nanoclusters.* J. Am. Chem. Soc., 2012. **134**(40): p. 16662-70.
53. Wu, Z., et al., *Aurophilic Interactions in the Self-Assembly of Gold Nanoclusters into Nanoribbons with Enhanced Luminescence.* Angew. Chem. Int. Ed. Engl., 2019. **58**(24): p. 8139-8144.
54. Jadzinsky, P.D., et al., *Structure of a Thiol Monolayer–Protected Gold Nanoparticle at 1.1 Å Resolution.* Science, 2007. **318**: p. 430-433.

55. Parker, J.F., et al., *The Story of a Monodisperse Gold Nanoparticle: Au25L18.* Acc. Chem. Res., 2010. **43**: p. 1289-1296.
56. Yang, T.-Q., et al., *Origin of the Photoluminescence of Metal Nanoclusters: From Metal-Centered Emission to Ligand-Centered Emission.* Nanomaterials, 2020. **10**(2): p. 261.
57. Luo, J., et al., *Aggregation-induced emission of 1-methyl-1,2,3,4,5-pentaphenylsilole.* Chem. Commun., 2001(18): p. 1740-1741.
58. Hong, Y., J.W.Y. Lamab, and B.Z. Tang, *Aggregation-induced emission.* Chem. Soc. Rev., 2011. **40**: p. 5361–5388.
59. Chen, Y., et al., *Aggregation-induced emission: fundamental understanding and future developments.* Mater. Horiz., 2019. **6**(3): p. 428-433.
60. Liao, P., et al., *Clusterization-triggered emission (CTE): one for all, all for one.* Mater. Chem. Front., 2021. **5**(18): p. 6693-6717.
61. Zhang, H., et al., *Clusterization-triggered emission: Uncommon luminescence from common materials.* Mater. Today, 2019.
62. Goswami, N., et al., *Luminescent Metal Nanoclusters with Aggregation-Induced Emission.* J. Phys. Chem. Lett., 2016. **7**(6): p. 962-75.
63. Wu, Z., et al., *Unraveling the Impact of Gold(I)–Thiolate Motifs on the AggregationInduced Emission of Gold Nanoclusters.* Angew. Chem. Int. Ed., 2020. **59**: p. 9934 –9939.
64. Sugiuchi, M., et al., *Aggregation-Induced Fluorescence-to-Phosphorescence Switching of Molecular Gold Clusters.* J. Am. Chem. Soc., 2017. **139**(49): p. 17731-17734.
65. Yang, T., et al., *Interfacial Clustering-Triggered Fluorescence–Phosphorescence Dual Solvoluminescence of Metal Nanoclusters.* J. Phys. Chem. Lett., 2017. **8**(17): p. 3980-3985.
66. Yang, T., et al., *P band intermediate state (PBIS) tailors photoluminescence emission at confined nanoscale interface.* Commun. Chem., 2019. **2**(1): p. 1-11.
67. Peng, B., et al., *Physical Origin of Dual-Emission of Au–Ag Bimetallic Nanoclusters.* Front. Chem., 2021. **9**: p. 756993.
68. Yang, T.-Q., et al., *Caged structural water molecules emit tunable brighter colors by topological excitation.* Nanoscale, 2021. **13**(35): p. 15058-15066.
69. Zhou, J., et al., *Structural Water Molecules Confined in Soft and Hard Nanocavities as Bright Color Emitters.* ACS Phys. Chem. Au, 2021. **https://doi.org/10.1021/acsphyschemau.1c00020**.
70. Ewles, J., *Water as an Activator of Luminescence.* Nature, 1930. **125**: p. Water as an Activator of Luminescence.
71. Przibram, K., *Fluorescence of Adsorbed Water.* Nature, 1958. **182**: p. 520-520.
72. Cha, S.-H., et al., *Preparation and Photoluminescent Properties of Gold(I)-Alkanethiolate Complexes Having Highly Ordered Supramolecular Structures.* Chem. Mater., 2007. **19**: p. 6297–6303.
73. Goulet, P.J.G. and R.B. Lennox, *New Insights into Brust-Schiffrin Metal Nanoparticle Synthesis.* J. Am. Chem. Soc., 2010. **132**: p. 9582-9584.
74. Chen, T., et al., *Synthesis of thiolate-protected Au nanoparticles revisited: U-shape trend between the size of nanoparticles and thiol-to-Au ratio.* Chem. Commun., 2016. **52**(61): p. 9522-5.
75. Wu, M., et al., *Luminescent Au(I)–Thiolate Complexes through Aggregation-Induced Emission: The Effect of pH during and Post Synthesis.* J. Phys. Chem. C, 2019. **123**(10): p. 6010-6017.
76. Chang, H.Y., et al., *The effect of ligand-ligand interactions on the formation of*

photoluminescent gold nanoclusters embedded in Au(i)-thiolate supramolecules. Phys. Chem. Chem. Phys., 2017. **19**(19): p. 12085-12093.

77. Lin, H., K. Imakita, and M. Fujii, *Reversible emission evolution from Ag activated zeolite Na-A upon dehydration/hydration.* Appl. Phys. Lett., 2014. **105**: p. 211903.
78. Coutiño-Gonzalez, E., et al., *Thermally activated LTA(Li)–Ag zeolites with water-responsive photoluminescence properties.* J. Mater. Chem. C, 2015. **3**(45): p. 11857-11867.
79. Baekelant, W., et al., *Shaping the Optical Properties of Silver Clusters Inside Zeolite A via Guest-Host-Guest Interactions.* J. Phys. Chem. Lett., 2018. **9**(18): p. 5344-5350.
80. Aghakhani, S., et al., *Atomic scale reversible opto-structural switching of few atom luminescent silver clusters confined in LTA zeolites.* Nanoscale, 2018. **10**(24): p. 11467-11476.
81. Hoffmann, R., *Interaction of orbitals through space and through bonds.* Acc. Chem. Res., 1971. **4**(1): p. 1-9.
82. Grabowski, S.J., *What Is the Covalency of Hydrogen Bonding?* Chem. Rev., 2011. **111**(4): p. 2597-2625.
83. Hu, X.-D., et al., *Interfacial Hydroxyl Promotes the Reduction of 4-Nitrophenol by Ag-based Catalysts Confined in Dendritic Mesoporous Silica Nanospheres.* J. Phys. Chem. C, 2021. **125**(4): p. 2446-2453.
84. Shan, B.Q., et al., *Surface electronic states mediate concerted electron and proton transfer at metal nanoscale interfaces for catalytic hydride reduction of -NO2 to -NH2.* Phys. Chem. Chem. Phys., 2021. **23**: p. 12950-12957.
85. Tao, R., et al., *Surface Molecule Manipulated Pt/TiO2 Catalysts for Selective Hydrogenation of Cinnamaldehyde.* J. Phys. Chem. C, 2021. **125**(24): p. 13304-13312.
86. Bao, X., *Fundamental research in catalysis with emphasis on confinement effects.* SCIENTIA SINICA Chimica, 2012. **42**(4): p. 355-362.
87. Schmidbaur, H. and A. Schier, *A briefing on aurophilicity.* Chem. Soc. Rev., 2008. **37**(9): p. 1931-51.
88. Jansen, M., *Homoatomic d10–d10 interactions and their influence on the structure and properties of matter.* Angew. Chem. Int. Ed. Engl., 1987. **26**: p. 1098.
89. Brust, M., et al., *Synthesis of Thiol-derivatised Gold Nanoparticles in a Two-phase Liquid-Liquid System.* J. Chem. Soc., Chem. Commun.,, 1994. **7**: p. 801-802.
90. Geim, A.K., *Exploring Two-Dimensional Empty Space.* Nano Lett., 2021. **21**(15): p. 6356-6358.
91. Fumagalli, L., et al., *Anomalously low dielectric constant of confined water.* Science, 2018. **360**: p. 1339-1342.